Vol. 39, No. 4 (2017) 415-430, DOI: 10.24874/ti.2017.39.04.01

Tribology in Industry

www.tribology.fink.rs

RESEARCH

Numerical Modeling of Rough Contact between Two Cylinders with Axes Parallel

M.B.A. Aidoudi[a], J. Bessrour[a]

[a] *University of Tunis El Manar, National Engineering School of Tunis, Applied Mechanics and Engineering Laboratory, BP 37, El Belvedere, 1002, Tunis.*

Keywords:

Contact mechanics
Rough cylindrical surface
Microgeometry
Sum surface
Elastic-plastic
Gaussian surface
Finite Element Analysis

Corresponding author:

Malak Ben Attia Aidoudi
University of Tunis El Manar, National Engineering School of Tunis, Applied Mechanics and Engineering Laboratory, BP 37, El Belvedere, 1002, Tunis.
E-mail: MalakBenAttiaAidoudi@enit.rnu.tn

A B S T R A C T

The present paper represents a study of the effect of surface roughness in elastic-plastic micro contact between two cylinders in contact along their external generatrix by finite element analysis. This is the first study in the micro-scale geometry to analyze this particular contact used in industrial problem of fluid heat tracing. Two types of frictionless contact are investigated numerically. One examines the contact between two random rough cylindrical surfaces with Gaussian statistics for different topographies. The other proposed the contact between sum cylindrical surface which include the roughness and the elasticity of the both rough surfaces into contact, with perfectly smooth rigid cylindrical surface. The construction of sum surface is used in order to simplify the problem of rough contact. A full description of the method and the technical of construction of sum surface is presented. As a result, it was fund a good agreement between the two models. A multiple contact configuration was analysed in the form of cylindrical surface. Numerical results obtained under elastic conditions were also validated by comparison with theoretical solution of Hertz. A sensitivity analysis is presented in order to estimate the random draw of parameters on the results. We present then results showing the effects of roughness on contact parameters. Overall, it is found that the contact parameters are quite sensitive to the roughness parameters in elastic and plastic deformation. Results show that the surface topography has a large influence on the real area of contact. As a result of that, the real contact area ratio increases with the increasing of the displacement until it reaches a maximum limit value on elastic-plastic deformation. This value, less than unity, decreases with increasing roughness.

1. INTRODUCTION

The contact between two surfaces is a fundamental problem in contact mechanics. Indeed, it uses the fields of mechanical, thermal, wear and friction. It is also a multi-scale problem from microscopic to macroscopic phenomena effects. Many applications require understanding phenomena related to the contact. Among these applications, we are

interested in industrial problem of fluid heat tracing system. This common application in the process industry is used to maintain the full length of the pipe work at the required temperature. Heat tracing is simple in its operation principle, simple to install and very reliable. The hot fluid is usually contained in metallic tube or a small pipe attached to the pipe being traced (see Fig. 1). Heat transfer takes place through the line contact between the tracer and the pipe. The absence of roughness between heat source and pipeline allows very rapid heating. So the established heat flux depends directly on the assumed distribution of real area of contact between the two rough cylindrical surfaces subjected to a given mechanical load.

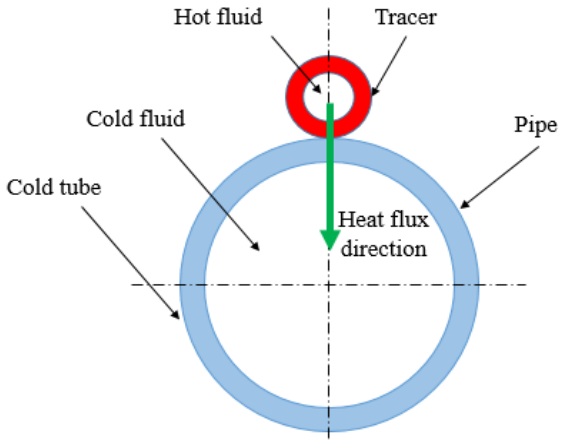

Fig. 1. Tracer heating principle.

In reality pipes are rough to some degree. The modeling of the real contact between the two tubes is a very important. The literature has practically no relative study to this particular contact problem. To study this type of contact problems, the characterization of roughness is necessary. Several models in the literature are available to describe the statistical and the numerical analysis of rough surface contact problems. A literature review reveals that many approaches are available to predict characteristics of contact between rough surfaces [1-6]. Statistical approaches are limited due to the very restrictive assumptions about random surface. The most successful models in literature were introduced by Greenwood and Williamson in 1966 [7]. They described the rough surface as consisting of spherical bumps of equal radius of curvature and with a Gaussian distribution of heights. This GW model uses the classical Hertzian solution [8] to stochastically model the contact between nominally flat surfaces. Then Greenwood and Tripp [9] showed that the contact between two rough surfaces could be treated by the contact between an equivalent rough surface and a smooth plan. Other works [10-13] used to extend the Greenwood and Williamson model to account asperities shaped dishes, elliptical, elastic-fully plastic deformation of asperities, or anisotropic surfaces. In all cases, the linear relationship between the contact area and the applied load was obtained. Because real surfaces would generally have a multiscale characters, it appears that the statistical parameters used are not unique but depends on the measurements parameters of surface roughness, such as resolution of the acquisition device or sampling length [14]. In this respect, Persson et al. [15] have developed a stochastic model that excludes the priority of any roughness scale. F. Robbe-Valloire et al. [16] study the elastoplastic deformation of nominally flat rough interface, they determined the global load and real area contact of two rough surfaces for a given separation between them. These models do not predict the deformed geometry of rough surfaces in contact and they used a non-standardized parameters. Hence the idea of F. Robbe-Valloire's to adopt a description of random microgeometry using ISO 12085 standard parameters [17]. With this method, signal processing is obtained by a graphic technique and use the motif concept defined as a part of profile which lies between two significant peaks [18-19]. Belghith and co-workers developed a new method for modeling rough contact between two flats surfaces using homogenization technique [20]. They used micro-geometrical characterization of rough surfaces given by F. Robbe-Valloire. Their model incorporates the behavior of irregularities and the fact that they must be elastic, elastic-plastic or fully plastic. They have been validated the use of the concept of sum surface in the case of contact between two random and rough flats surfaces. With the evolution of computer tools, many deterministic numerical models have been developed. Among the most robust methods, we find numerical methods in finite element analysis. These include the works of Hyun et al. [21] who considered a fully three dimensional finite element analysis for elastic contact between rough surfaces with fractal scale. L. Pei et al. [22] extended the findings of elastic contact to study the elastic-plastic phase considering a wide range of self-affine surface topographies. Sahoo and

Ghosh [23] have studied a fractal surfaces by means of commercial finite element software ANSYS. Unfortunately, these methods are limited by the size of the system to solve. To decrease this, other alternative numerical methods have been developed. These methods, called semi-analytical, assume that if the contact area is small compared to the size of the body and the slopes of the surfaces are low, the body can be treated as semi-infinite mass [24]. B. Buchner et al. [25] proposed a statistical method using the basic model introduced by Abbott and Firestone [26]. Based on this description, they deduced that the real area of contact varies linearly with load. For high pressure, it tends progressively to apparent area. In addition, among other numerical techniques to solve the problems of contact between rough surfaces, there is for example the Fast Fourier Transform. In particular, W. Peng and B. Bhushan [27] have used this technique to study the interfacial elastoplastic contact between a multilayered surface and a rough surface. M. Ciavarella et al. [28] tested numerically the validity of the Majumdar theory [29] and Persson contact [30,31] between fractal surfaces using Fourier and Weierstrass random series. Both theories underestimate the actual contact area in regions where the effort is relatively low. On the other hand, for relatively large efforts a good agreement between the results was found. Almqvist [32] also compared the theory of contact mechanics to Persson [30,33,34] at three numerical approaches which are Boundary Element Method, Green's function Molecular Dynamics and Smart Blocks Molecular Dynamics. D. Goerke et al. [35] simulated elastoplastic contact between two fractals surfaces. They have shown that the increase in surface hardness causes a decrease in the real contact area. The simulation also showed that waviness causes a reduction of the normal stiffness of the contact. Later, another approach has been proposed by M.B. Amor et al. [36] to analyze numerically the combined effect of roughness and deformation mode, purely elastic or elastic-plastic, on the contact performances. The effect of roughness on the Von Mises and the residual stress after the unloading process is also shown. Thermal and mechanical analysis should be fully coupled and conducted simultaneously. An overview of thermoelastic contact studies has been given in [2]. Chen and Wang [37] developed a three-dimensional thermoelastoplastic contact model for a sliding contact of a half-space over a stationary elastic-plastic sphere. In this model, the effects of steady state heat flux, temperature-dependent strain hardening behavior and interaction of mechanical and thermal loads were taken into account. They also developed in [38] the transient contact model which takes into account transient heat flux at the sliding interface.

The motivation for the present study comes from non-existence of the thermal contact solution between the tracer and the pipe to be heated. This thermal problem cannot be solved if we don't address the mechanical contact problem to identify the contact area from an imposed load. In this paper, we present a new study of numerical modelling of mechanical frictionless micro contact between rough random cylindrical surfaces with axes parallel. The article begins with an overview of analysis concerning smooth and rough external contact. First, we compare the results obtained under elastic conditions were with theoretical solutions. Afterwards, we consider the effect of roughness in cylindrical contact presenting the contact of four classifications of roughness (N3, N4, N5 and N6). First study is based on standardized roughness parameters ISO 4287 [39] to study the effect of roughness on contact. A sensitivity analysis is also presented to study the impact of the random draw of roughness parameters on real contact area. Subsequently, by application of the motif procedure to cylindrical surface, a second study is carried out in which the contact between rough-rough cylindrical surface is transformed into a contact between smooth rigid surface and a sum surface using "motif" ISO procedure [40]. Then we compare the results with those provided from sum surfaces in the case of two-dimensional microscopic contact between rough cylinders with axes parallel. Commercial finite element software Abaqus is the base of our simulation where two dimensional rough surfaces are generated in Matlab.

2. CONTACT MODELS BETWEEN TWO ELASTIC CYLINDERS

2.1 Analysis of Smooth contact

The research on smooth contact parameters began with the pioneering work of Hertz [8] in 1881. He considers the frictionless contact between two cylinders with their axes parallel pressed together by a force as shown in Fig. 2.

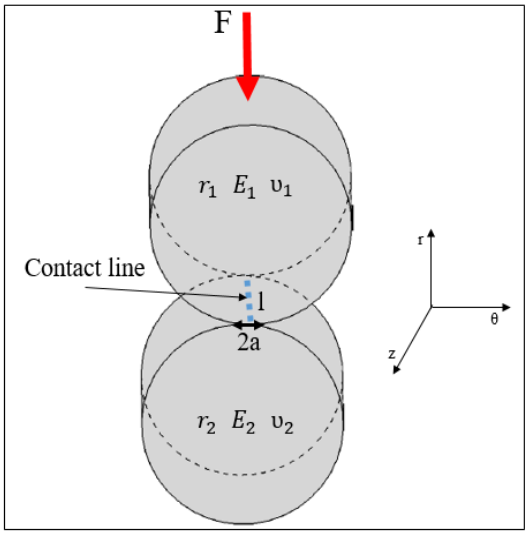

Fig. 2. Schematic illustration of elastic contact between two parallel cylinders.

Hertz found that when the load is applied, the initial line contact zone forms a band in the direction of the axis's half-width (*a)* and the contact pressure increases linearly with the characteristic dimension of the elastic contact zone.

The expression for the semi contact length and the maximum contact pressure are given by:

$$a = \sqrt{\frac{4Fr}{\pi E^*}} \tag{1}$$

$$P_{\max} = \sqrt{\frac{FE^*}{\pi . r}} \tag{2}$$

Where F is the concentrated load applied in the center of each cylinder, r and E^* are the reduced radius of contact and the contact modulus defined by:

$$\frac{1}{r} = \frac{1}{r_1} + \frac{1}{r_2} \tag{3}$$

$$\frac{1}{E^*} = \frac{1-\nu_1^2}{E_1} + \frac{1-\nu_2^2}{E2} \tag{4}$$

Where: r_1 and r_2 are the radii of the solids, E_1 and E_2 their elastic moduli, ν_1 and ν_2 their corresponding Poisson ratios.

If the starting position is a line Hertzian contact *(l)*, the area of contact varies as the square root of the applied force F is given by:

$$A \infty \sqrt{F} \tag{5}$$

2.2 Analysis of Rough contact

In mechanical contacts, generally we consider a contact between two topographically smooth bodies to determine the relation between the applied load, the contact area and the contact stresses. But in reality surfaces are not perfect and the contact occurs on the tops of the asperities. It is therefore necessary to define the parameters of contact for a rough contact. This type of contact is very difficult to perform because of the complications introduced. To simplify this contact problem, the so-called sum surface is defined and the type of rough-rough contact is returned to the contact between a perfect smooth rigid surface and a sum rough deformable one (Fig. 3).

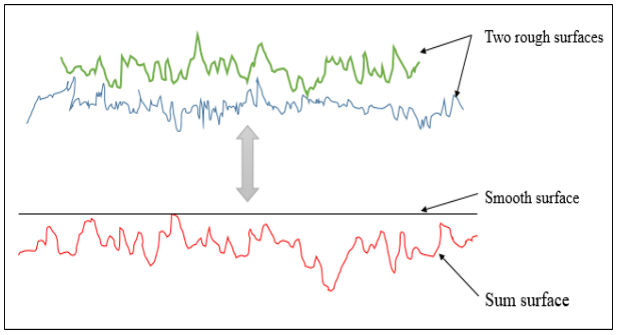

Fig. 3. Construction of the sum surface between two flat surfaces.

The sum surface combines both the microgeometry aspects of both rough surfaces and the deformability of the two materials constituting each of their parts. Greenwood and Tripp [9] shows that the contact between two rough surfaces can be modeled by the contact between a flat surface and an equivalent rough surface characterized by a curvature of asperity which is the same of the curvature of asperities of the two surfaces.

The sum surface has to combine the elasticity of both surfaces. The classical relation (4) is used. Concerning the plasticity of sum surface, the lowest values of the yield stress of each material in contact is assigned.

It is possible to obtain the sum surface using three kinds of relations [16]:

i. Relation for mean-type roughness parameter

$$R = R_1 + R_2 \tag{6}$$

ii. Relation for root mean square-type parameter

$$SR = \sqrt{SR_1^2 + SR_2^2} \quad (7)$$

iii. Relation for distance-type parameter

$$AR = \frac{1}{2}(AR_1 + AR_2) \quad (8)$$

This relation has been used by F. Robbe Valloire [18-20] based on the concept of so-called motif [17] defined as that part of profile bound between two peaks (see Fig. 4).

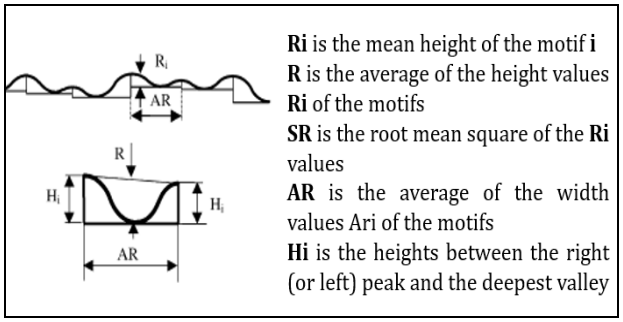

Fig. 4. Geometrical characteristics of a motif.

A few studies were conducted to describe and develop the construction methodology of microgeometry of the sum surface. We note an entire absence of any study of rough contact using the concept of sum surface between two cylinders with axes parallel.

Therefore, the aim of the next part of our study is to use the assumption presented previously to construct the sum surface between two rough cylindrical surfaces. We maintain the same interstice between the two mean surfaces. This interstice is called overclosure, we defined it as the gap opening between rough surfaces dependent of the actual distance between the mean surfaces on the main axis of the two cylinders (Fig.5).

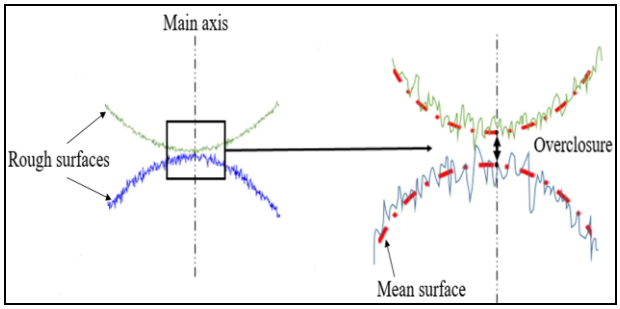

Fig. 5. Overclosure defined between two rough cylindrical surfaces.

Subsequently, we compare the two approaches: rough-rough contact and sum surface - smooth contact between surfaces in the range of average roughness R_a framed by 0.05 and 0.45 µm. But at first, we study the effect of roughness on mechanical parameters.

We will ignore the multi-scale character. We consider only the micro-geometric scale and we neglect waviness profile.

3. MODEL DESCRIPTION OF MICRO ROUGH CONTACT

3.1 Statistical and numerical model

With the staggering growth of some computational models, using a finite element analysis software to model the roughness is a great interest to study the rough contact between two surfaces. In the case of rough contact, the contact occurs only at some highest asperities that have only a small proportion of the real contact area. Under the plane strain hypothesis, a two dimensional models has been developed between two cylinders using a software for finite element analysis with the mode of elastic-plastic deformation (Fig. 6).

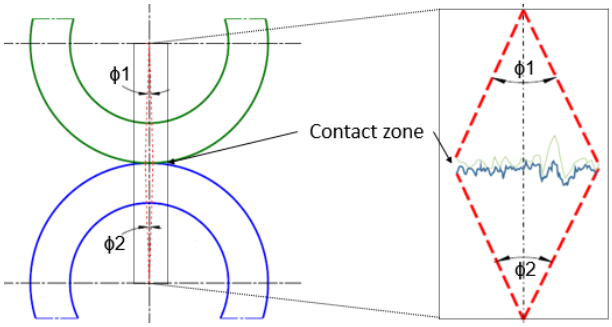

Fig. 6. Angle of sector contact.

Where: φ_1 and φ_2 presents the angle of the two sectors of rough cylinders in contact.

- Geometric description of random topography

We shall use a contact problem between two cylinders in *(r, ϴ)* plan. The first step is to define the surface roughness. The rough profile was generated in Matlab with random function and imported to Abaqus using python script. The microgeometry of the rough surface is defined by the amplitude parameters of the main standard method ISO 4287 [37]. We use a

Gaussian symmetric distribution for the asperity of each generated profile that is given as:

$$\phi(z_s) = \frac{c}{\sigma_s} e^{-z_s/\sigma_s} \quad (9)$$

Where: c is an arbitrary constant and z_s is an amplitude parameter of the asperities summit height distribution.

We consider that the Root Mean Square R_q and the Average Roughness R_a are proportional [41] such as $R_q \approx \sqrt{\frac{\pi}{2}} R_a$.

The Figure 7 represents an example of roughness profile obtained following a random selection of the roughness parameters R_a (arithmetic average), R_q (variance), R_{sk} (Skewness) and R_{ku} (Kurtosis) which respectively correspond to the first moment m_1, the second moment m_2, the third moment m_3 and the fourth moment m_4.

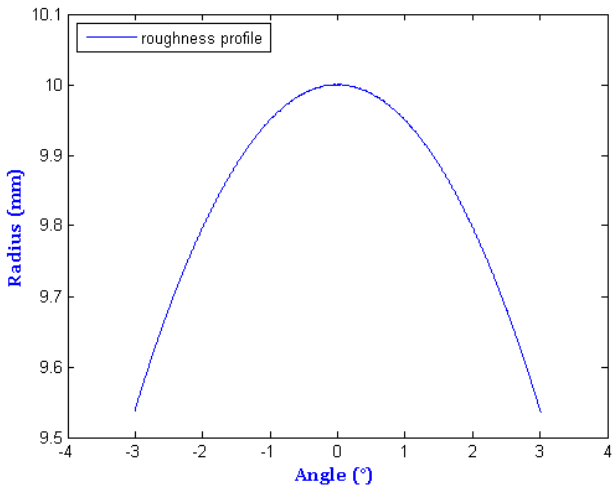

Fig. 7. Example of Profile of rough surface (m_1= 0.38 µm, m_2=0.47 µm m_3=0, m_4=3).

Numerical model

We develop the microscopic numerical model to study the frictionless contact between two rough cylindrical surfaces with their axes parallel. The study is limited to look into the contact between two angular sectors. Figure 8 show dimensions of geometric study.

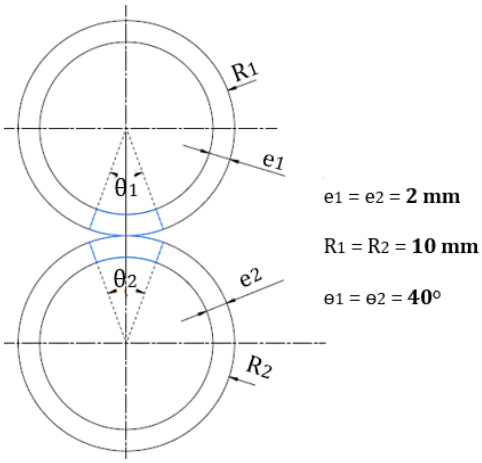

Fig. 8. Geometry and dimensions used in the present study.

Element finis mesh

A linear quadrilateral plane stress element mesh (CPS4R) is used to mesh the surface. The cylinder is divided into three different mesh density zones (Fig. 9). The zone closer to the contact surface had the finest mesh to represent the complicated geometry of rough surface and to capture high stress gradients in the zone close to the surface. The other zones had gradual coarser mesh at increasing distance from the rough surface.

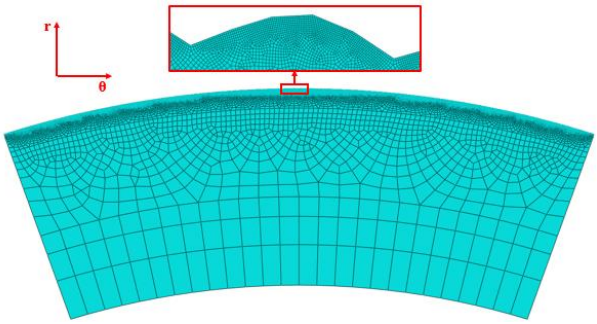

Fig. 9. Finite Element mesh used to describe the contact.

Each zone is divided into many discrete elements. This approximation of the model geometry introduces inherent numerical error into the finite element solution. This error should decrease with increasing mesh density for a robust finite element model as contact parameters converge to a final value. It is also desirable to balance model accuracy with required solution time. Consequently, a convergence study was performed to determine an adequate mesh size for the finite element model.

Boundary conditions

The boundary conditions are shown schematically in Fig. 10. A normal displacement of 15 µm is prescribed on the top surface of the upper cylinder. The lower cylinder is taken as reference. A total blockage of the movement of the nodes located on the bottom facet.

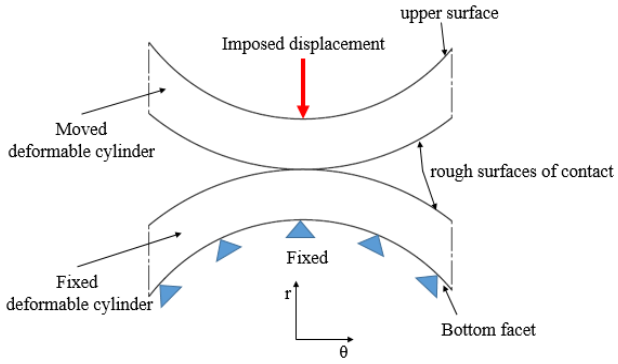

Fig. 10. Schematic representation of boundary conditions.

The two cylinders are assumed deformable. We assumed that it exists no third body in the interface which can transmit load.

Material properties

For the present study, the API 5L X65 steel [42] is chosen, which is popularly used for gas pipelines widely used by the industry. The material data for the investigated steel were determined by means of tensile tests [43]. The corresponding flow curve is presented in Fig. 11.

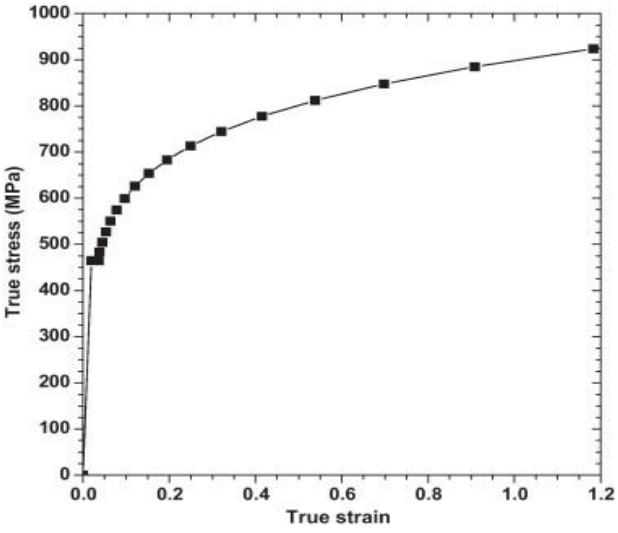

Fig. 11. True stress-strain curve of API 5L-X65 steel.

The X65 steel was characterized as isotropic and homogeneous across the cross-section, with hardening elastic-plastic behavior being present in the material. Tensile properties of the present API X65 steel are summarized in Table 1.

Table 1. Tensile properties of the API X65 steel.

Young's modulus **(Gpa)**	Poisson's ratio	Yield strength **(Mpa)**
210.7	0.3	464.5

3.2 Contact between smooth and sum surface

As described previously in paragraph 2.2, in most research, the calculation of contact rough-rough contact between two deformable surfaces is transformed into contact between a rigid smooth and sum rough surface (Fig. 12). We have applied and validated this methodology in the case of cylindrical surfaces to simplify the rough-rough contact problem. The basic principle consists in conserving the same initial overclosure between rough surfaces (Fig. 5). The microgeometric parameters of each surface are combined to obtain the parameters of the sum surface. The sum surface is well defined through the game of the following parameters: Young's modulus E^*, Poisson's ratio υ, the average of the height values R, the root mean square SR and the average of the width values AR.

The isotropic sum surface depends only on the geometry of the starting surface. As starting rough surfaces, sum surface has a Gaussian statistical distribution of the altitude of the peak.

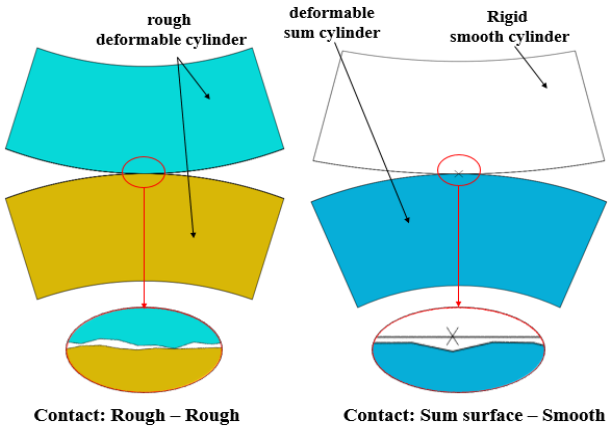

Fig. 12. The contact zone.

Roughness parameters for numerical study

Statistical description of isotropic random surface is applied to a large range of microgeometries classified according to their

average arithmetic roughness R_a ranging from 0.05 to 0.45 µm. Both rough cylinders in contact belongs to the same roughness class (N3, N4, N5 and N6).

This work aims to construct an equivalent sum surface from two cylindrical rough surfaces in order to compare the results of rough–rough contact and sum surface–rigid smooth contact with random surfaces for the same load. Our study will be limited to use the same micro geometrical assumptions and mechanical as that used for the calculation between two rough flat surfaces [18,20].

The two-dimensional surface parameters for the surfaces of numerical study are summarized in Table 2.

Table 2. Micro-geometrical parameters of rough surfaces using in current work.

	Parameters (µm)	Class (N3)	Class (N4)	Class (N5)	Class (N6)
Amplitude parameters	R_{a1}	0.05	0.12	0.22	0.4
	R_{q1}	0.06	0.15	0.27	0.5
	R_{a2}	0.08	0.18	0.3	0.45
	R_{q2}	0.1	0.22	0.37	0.56
Motif parameters (surface 1)	R	0.09	0.19	0.26	0.34
	SR	0.14	0.15	0.19	0.21
	AR	4.71	3.73	3.25	3.09
	SAR	3.69	1.85	1.51	1.29
Motif parameters (surface 2)	R	0.12	0.21	0.35	0.53
	SR	0.13	0.15	0.21	0.31
	AR	3.32	3.14	2.90	3.09
	SAR	1.74	1.33	0.96	1.41
Motif parameters (sum surface)	R	0.22	0.39	0.62	0.88
	SR	0.20	0.22	0.28	0.38
	AR	4.02	3.43	3.07	3.09
	SAR	4.08	2.28	1.79	1.91

4. RESULTS AND DISCUSSION

4.1 Smooth contact

Mesh convergence study

For each number of elements, real area of contact is observed. The results are shown in Fig 13.

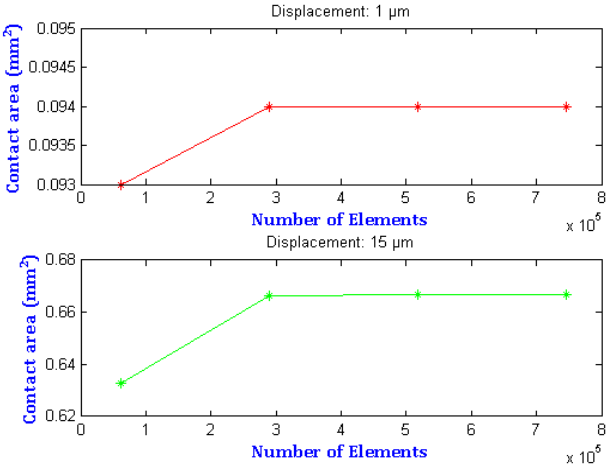

Fig.13. Mesh convergence study results.

The area does not vary significantly over the range of mesh sizes studied, and the finite element solution is considered to be sufficiently converged to a certain critical size.

Consequently, 745 276 elements are chosen for appropriate model accuracy and reasonable solution time (see Fig. 9).

Hertz elastic solution

In order to validate the application of the model to multiple contact with different roughness class, results obtained assuming elastic behavior of smooth surface have been compared with the corresponding solution of Hertz [8]. Both the analytical and finite element models were applied to cylinders with inner and outer radii of 8 mm and 10 mm, respectively (Fig. 8). A comparison of contact area from the elastic simulation with the analytical equation (1) is shown in Fig. 14.

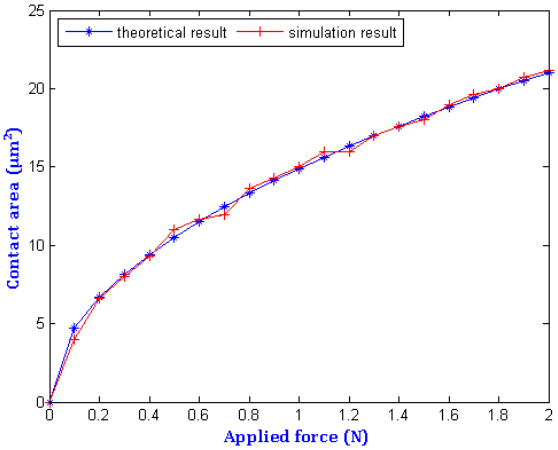

Fig. 14. Comparison of Hertzian area obtained from the FE model with theoretically calculated values.

The figure (Fig. 14) show that finite element method under elastic conditions is in good agreement with analytical Hertz solution. Results has never been obtained before in the case of cylindrical surfaces. From the obtained results, we can be seen that the numerical results give very exactly data. Thus the numerical approach can be used for the solving of the rough cylindrical problem with very well accuracy of results.

4.2 Rough contact

Normal distribution of results

The model then extended to include plastic behavior. In order to further increase confidence in the software under elastic-plastic condition, statistical study was carried out. The contact between two rough cylindrical surfaces is analysed as a random process by modeling the two-dimensional rough surface as an isotropic, Gaussian, random variable. The rough profile is defined from a random variable characterized by a given parameters which are the arithmetic average R_a, the root mean square R_q, the Skewness R_{sk} and the Kurtosis R_{ku} (see paragraph 3.1). The simulation study can include a sensitivity analysis to a set of inputs parameters. The contact parameters are distributed randomly over the rough surface and its probability density function changes with normal displacement. So it's possible to approximate the mean value and the standard deviation of contact parameters between rough-rough contacts.

The objective of this section is to prove that contact parameters can be averaged by an average value (μ) and a standard deviation (σ) during the loading. For each value of the imposed displacement, the calculations were performed for ten surface created for every roughness class.

The mean and standard deviation of the resulting contact parameters were calculated. Ten random pinning are used for sensitivity analysis. Figure 15 shows evolution of real contact area for medium (N3) and very rough surface (N6). These simulations were carried out with the same parameters of roughness.

Noting that random points are very close to each other and concentrated around an average value.

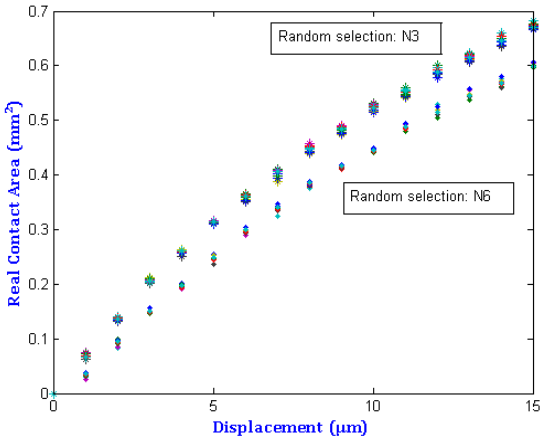

Fig. 15. Sensitivity of real contact area to the random pinning of roughness profile.

These values can be approximated by Gaussian curve. Figure 16 shows the probability density function of the distribution of real contact area for the two classes of roughness (N3 and N6) and two displacements (u=6 µm and u =15 µm). Data points forms a normal distribution centered directly under their entrance point. We can assume that real contact area can be approximated by a mean value for each imposed displacement.

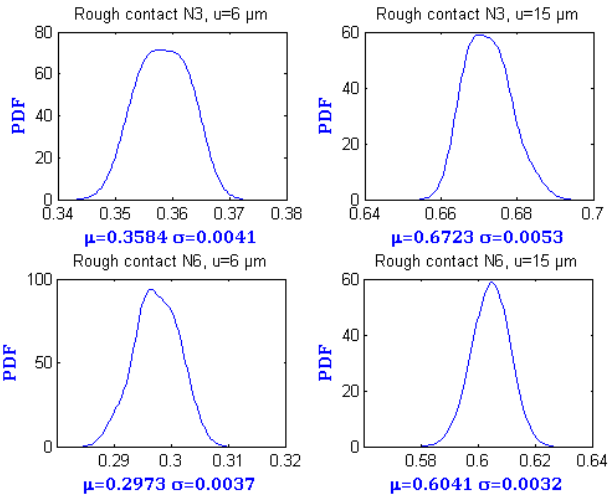

Fig. 16. Probability density distributions of real contact area.

The result in the next section are obtained by averaging the contact parameters value (ten profiles are simulated and simply the mean values are shown).

Results with rough surface

Present section predict surface contact parameters (contact area, contact force, overclosure...) and hence the plastic strain where

these will all vary with applied displacement, material properties and surface roughness. Four random rough contacts with different surface roughness are simulated. Roughness microgeometry values are classified according to their arithmetic average roughness R_a:

- Class N3 for the medium rough surface R_a between 0.05 and 0.1 µm
- Class N4 for the slightly rough surface R_a between 0.1 and 0.2 µm
- Class N5 for the rough surface R_a between 0.2 and 0.4 µm
- Class N6 for the very rough surface R_a between 0.4 and 0.5 µm

It can be seen from the expression (5) that contact area between the two surfaces in the case of contact between two smooth cylinders with axes parallel is proportional to the square root of the applied load which is verified here Fig. 17. For medium rough surface (N3), the evolution of real contact area has also the same shape of the curve. For rougher surfaces (N6), the real area changes almost linearly with load and it's slightly affected by the difference in topography. Results show very good agreement with Analytical [12,31] and Numerical solutions [44,45].

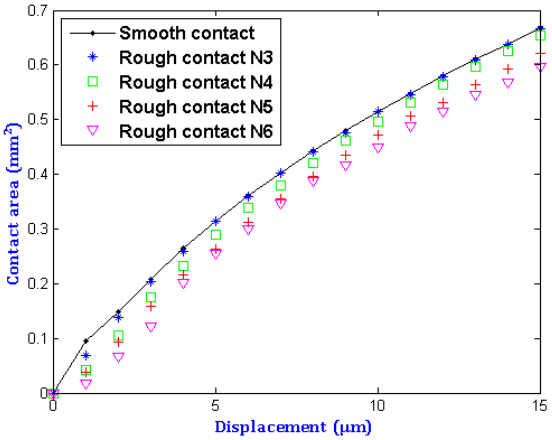

Fig. 17. Contact area versus imposed displacement for the contact between a smooth surfaces and rough surfaces with varying roughness.

The increasing roughness decreases the contact area. This is perfectly logical because for the rough surface, contact is limited to the asperity peaks. We note that, when the degree of surface roughness increases, the true contact area between cylindrical reduce for the same displacement. We check that smooth model naturally gives greater value of contact area than rough contact models as the Fig. 17 depicts.

The smooth contacts overestimate the contact area. Indeed, the increase in roughness of 0.1 to 0.5 µm involves a decrease of 16 % of the value of the contact area. In higher roughness, with microgeometry classification N5 and N6, the influence of displacement is stronger.

Another physical variable of interest in contact mechanics studies is the ratio r between the real area of contact and the nominal contact area (see Fig. 18). Analysis shows that the real area of contact is always smaller than the apparent area of contact, with the ratio between these two areas becoming closer to unity for smoother surfaces (classification N3). For this class, the ratio r increases too quickly with displacement. When the imposed displacement reaches 5 µm and beyond, the ratio reaches the limit value 99 %. Almost all off the contacting asperities are deformed. For the same displacement, r reaches 91 % for slightly rough surface (N4), 83 % for the rough surfaces (N5) and 80 % for rough surface (N6).

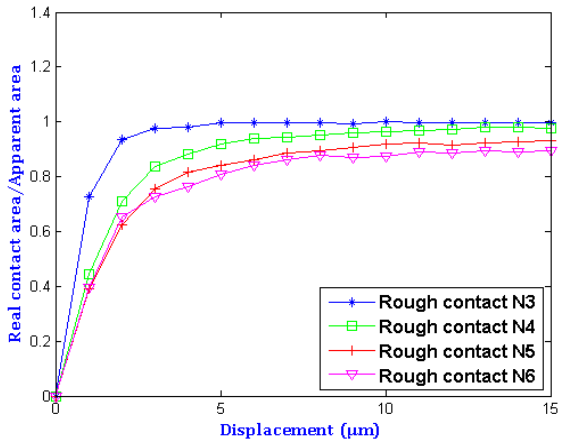

Fig. 18. The ratio of the real contact area of contact to the apparent area as a function of displacement for the four simulated surface roughness.

The evolution of the relationship between the overclosure formed by roughness heights defined in paragraph 2.2 and displacement is also analysed. Figure 19 shows the evolution of the overclosure for four roughness classes. As it was defined, overclosure is zero for perfect contact and as the surfaces becomes rougher, initial overclosure increase. Unstrained rough surfaces severely enhance an initial gap. Contact occurs at an increasing number of points and the

overclosure between the two mean surfaces is reduced until the asperities reach its equilibrium location. The position of this equilibrium point is determined from elastic- plastic theory. Overclosure tends toward zero beyond 5µm for the medium rough surface (N3). It can be observed that for very rough surface (N6) overclosure reaches 0.98 µm at the maximum displacement. The gap between the two rough surfaces is still large because there are unreformed asperities.

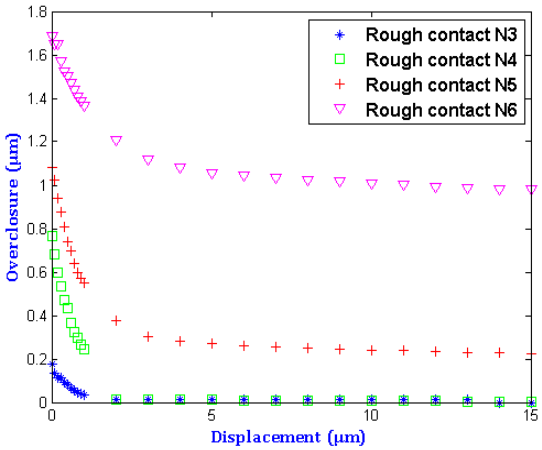

Fig. 19. Evolution of the overclosure as a function of displacement with varying roughness.

Force-displacement relationship in the mixed elastic-plastic regime is shown in Fig. 20. The force is assumed to be the summation of the contact force at each contact area. When the two surfaces become closer, contact force increase continuously as displacement increases.

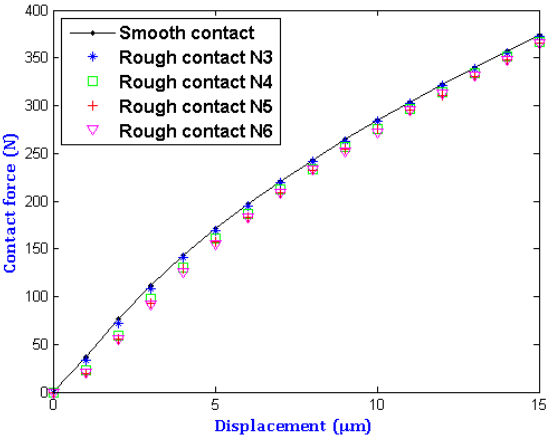

Fig. 20. Effect of roughness on contact force in cylindrical surfaces with varying roughness.

The nominal contact force on the apparent area reached approximately 374 N, it corresponds to a contact pressure of 560 MPa. For very rough surface, the contact force reaches 365 N when the imposed displacements reach 15 µm.

Contact angle can be affected by surface roughness. Curve of Fig. 21 connects the contact angle to the imposed displacement for four different surfaces.

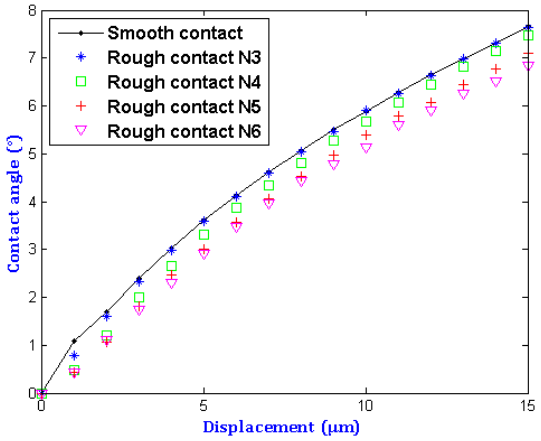

Fig. 21. Effect of roughness on contact angle in cylindrical surfaces with varying roughness.

Both predict a decrease in contact angle with increasing roughness class. The microscopic smooth model predicts a much greater percentage change in contact angle. There are about 10 % of reduction in contact angle between perfect surface and very rough surface (Classification N6).

Figure 22 shows the evolution of equivalent plastic strain as a function of displacement. These curves cover a region of the plastic strain value from 0 to 0.70.

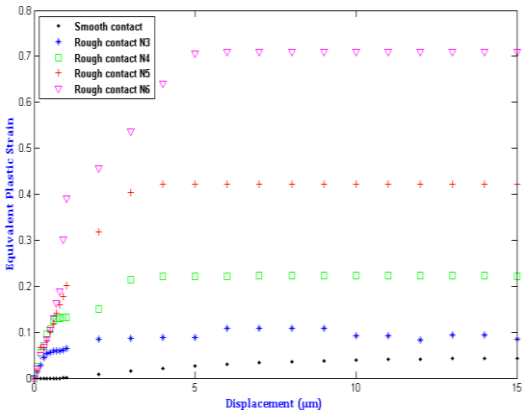

Fig. 22. Evolution of the maximum plastic strain as a function of displacement with varying roughness.

A large difference between the curves can be observed in the region 0.08 and 0.70 of plastic

strain. For smooth contact, the deformation is initially elastic. Therefore, the elasticity model of subsection 2.1 is applicable. The equivalent plastic strain exceeds the yield strength when displacements reach 0.8 µm. Before this value, plastic strain equals zero during the whole process of loading until the appearance of plasticity. For rough contact, plastic deformation exceeds the deformation corresponding to the elasticity limit. This does suggest, however, that the purely elastic model is increasingly inappropriate as roughness increases. High roughness surfaces introduce a local increase in the surface deformation, stress concentrations which may facilitate rupture of material if we increase more the displacement.

Figure 23 shows the disvalues of micro-displacement for five configurations of contact. Displacement varies locally especially around asperities. Imposed displacement generates a local micro displacement on the interface of contact. The node of asperity peaks of the top cylinder undergoes an important radial displacement that decreases away from the contact zone.

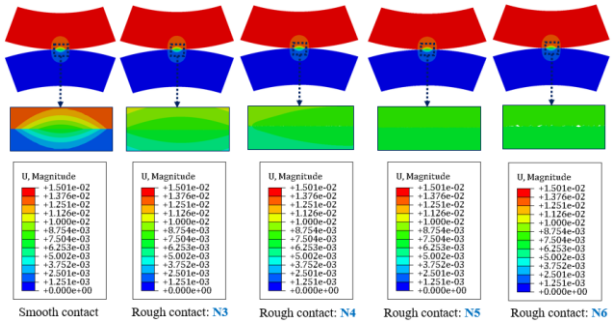

Fig. 23. Repartition of micro-displacement (mm) for smooth surfaces and four roughness class at the maximum displacement.

The Von-Mises equivalent stresses are depicted in Fig. 24. The result corresponds to the maximum displacement of 15µm. When surface is smooth, contact stress has an elliptical distribution across the contact angle. The maximum Von Mises stresses are reached below the contact area. This distribution is similar to those predicted by Hertzian theory [8]. As the contact load is increased beyond the elastic limit the stress distributions deviate from those predicted using purely elastic Hertzian theory, and the area of peak Von-Mises stress results in localized material yield. As the displacement is increased further, the plastic zone at the center of the contact grows. We note that, the maximum stress increases with increasing surface roughness average.

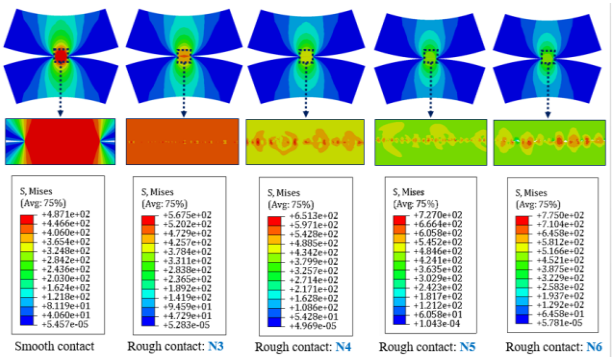

Fig. 24. Stress Contour Plot (MPa) at the Contact Zone for smooth surfaces and four roughness class at the maximum displacement.

Indeed, the maximum contact stress is located on the high asperity for rough surfaces, this is why the mesh in this region is refined adequately to describe these high stress gradients. The surface with the lowest roughness N3, presents maximum stress very close to the perfect contact with a maximum value of around 567 Mpa each lead to plastic deformation. The value is 464 Mpa for displacement 0.1 µm. Pressure distributions due to surface roughness in contact induce high stresses just beneath the surface [46].

The contact pressure along a distance in contact zone is also presented in order to know if nodes are in contact or not (Fig.25). If the contact pressure of a node is zero, then the node is still far off contact, but if not the node is in contact. As the displacement is increased, new contacts are created and existing contacts grow in size and may merge with neighboring contacts. As can be seen in Fig. 25, the contact pressures according to the four rough models are different from the smooth model. In the case of full contact, contact area is overvalued, so the contact pressure in the close contact area is very high at some local spots. In the case of rough contact, maximum contact pressure is in the highest peaks because the real microscopic contact in fact corresponds to a sum of contact between points. Contact with very rough surface (N6) results in a significant plastification. We see that the behavior becomes inherently more plastic as the roughness increases. It is much lower than in the case of contact with surfaces in Class N5. The maximum pressure is around of

1140 MPa for the very rough surface (N6) and 615 MPa for the medium one (N3).

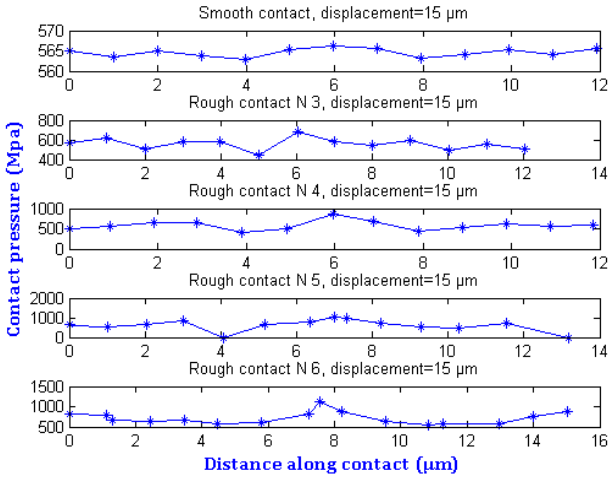

Fig. 25. Contact pressure distribution (MPa) in contact zone for smooth surfaces and four roughness class at the maximum displacement (15 µm) obtained from the FE analyses.

The contact pressure increases with increasing surface roughness. This result, already confirmed by C. Mayeur [24,46]. The behavior of asperity is initially elastic. As the displacement increase, the elastic behavior continues to describe the deformation until a critical displacement is reached. At this value and beyond the asperity deforms as purely plastic body and the strain magnitude increase.

The distribution of the equivalent plastic strain for the contact region is shown in Fig. 26.

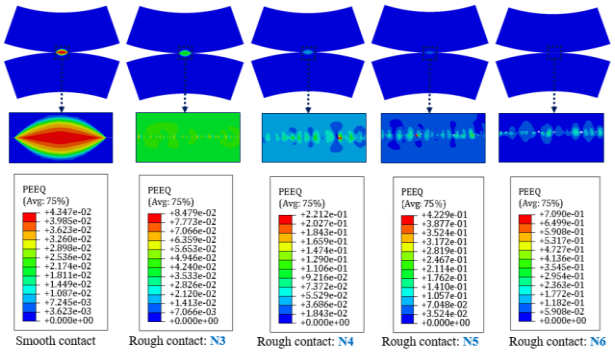

Fig. 26. Distribution of equivalent plastic strain for smooth surfaces and four roughness class at the maximum displacement.

Local plastic strain is height when surface is very rough. If the loading is increased further a damage of material can be obtained. It increases when surface roughness is increases. For the smooth contact, plastic strain is low and leads to the appearance of the maximum limit value of the real contact area ratio *r*.

4.3. Sum surface

The validation of the assumptions of the method of the sum surface in the case of a cylindrical contact is to verify that the rough-rough contact and smooth rigid–sum surface contact give equivalent results for the same boundary conditions, the same characteristics of the materials and the same mesh with the same initial overclosure.

From equation (4), the sum surface was supposed to be elastic with Young's modulus E_{eq} equal to 116 GPa.

We realized series of rough-rough and rigid smooth – sum surface contact simulations for the four roughness classifications. The validation of the passage is performed by comparing the evolution of the real contact area as a function of imposed displacement. Figure 27 shows the evolution of real contact area as a function of the normal displacement for different roughness class.

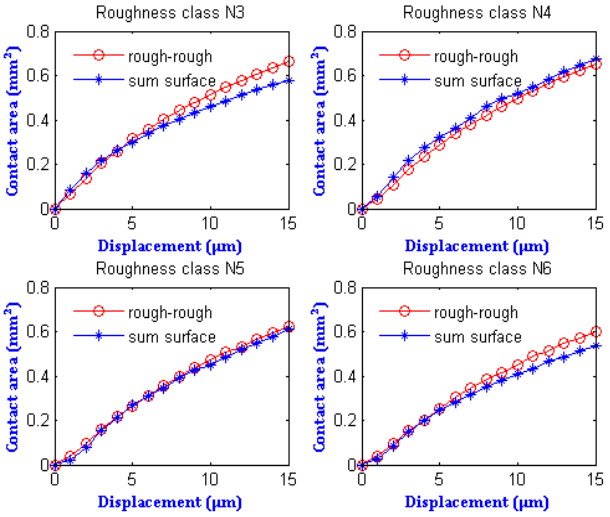

Fig. 27. Evolution of the real contact area: comparison between rough-rough surfaces and sum-smooth surfaces for four roughness classifications.

Results show that the sum surface predicts the similar behavior of the rough-rough contact area.

Once u = 10 µm is reached, a difference between the two curves can be observed for medium surface N3 and N6. This is due to the distribution of summit altitudes of sum surface which is not necessarily the conventional Gaussian

distribution. For the other class roughness, the difference is very less and a very good coincidence between the two curves is obtained.
The contact between two rough cylindrical surfaces is reproduced faithfully. These results led to validate the construction of sum cylindrical surface with the same approach used in the case of flat surfaces [16-20]. It is possible to ensure a perfect equivalence between the results of the two configuration of contact. This simulation confirms the validity of sum surface in the case of cylindrical surfaces with axes parallel on the micro geometric scale. This is further proof of the suitability of the numerical techniques discussed here to study the contact mechanics of elastic-plastic cylinders with randomly rough surfaces under engineering conditions.

5. CONCLUSION

The surfaces of several types of geometrical are irregular, but in many cases we simply limit the study to microgeometry defects. In this paper, we introduced the numerical microscopic study of elastic-plastic, homogeneous and isotropic contact between two random cylindrical rough surfaces. The model is statistical in nature. So that the calculated contact parameters such as contact angle, contact area and contact pressure are statistical. The numerical approach allows us to calculate not only the averages of these quantities, but also their standard deviations. This gives insight into the likely variations expected any contact parameters arising from the random nature of surface contact. This configuration of contact is used to represent two dimensional rough contacts between two tubes in the case of trace heating. This industrial application is used to maintain a constant flow temperature or to maintain process temperature. Heat transfer along pipe length between the tracer and the pipeline to be heated depends on the surface roughness. Especially, we had study the mechanical external contact between two cylindrical surfaces for four roughness classes (N3, N4, N5 and N6) over a wide range of roughness (R_a range from 0.05 to 0.45 μm).This to estimate the contact parameters as area, force, pressure, angle of real contact and overclosure which has been defined in the mean frontal plan of the two cylinders. First, we compared the numerical results obtained under elastic conditions with theoretical solution of Hertz. Then, we realized analysis sensitivity in order to know if the result is robust to changes in random draw of roughness parameters of ISO 4287, used to represent roughness profile, and if the tribological behavior at the interface cylinder-cylinder is influenced. Overall, it is found that the contact parameters are quite sensitive to the roughness parameters in elastic and plastic deformation. Results show that the surface topography has a large influence on the real area of contact. Therefore, the real contact area ratio increases with the increasing of the displacement until it reaches a maximum limit value on elastic-plastic deformation. This values, less than unity, decrease with decreasing roughness.

This is the first time this study in the case of cylindrical surfaces in reported in order to resolve the rough contact problem. The next step of our study was to switch from a rough-rough contact to a sum rough-rigid smooth contact. The motif parameters of sum surface are calculated using an algorithm that we developed using Matlab. The rough profile of sum surface was generated in Matlab and imported to Abaqus using python script. This transition using equivalent sum cylindrical surface was justified by comparing results of parameters of contact from different simulations of the four roughness classes of rough-rough contact and smooth rigid-sum surface. From this comparison, it's justified that the concept of the equivalent sum surface provides a good estimation of the contact between two rough cylindrical surfaces belonging to the same classification of roughness. The study validates the use of the FE code for elastic-plastic contact analyses of cylinder-cylinder and encourages investigation of other 2D surface contacts using this approach. And finally, this is further proof of the suitability of the numerical techniques discussed here to study the contact mechanics of elastic-plastic cylinders with randomly rough surfaces under engineering conditions.

It is hoped to extend the model to take account of the effects of rough surfaces on the contact parameters and to study the effects of non-Gaussian surface roughness on frictionless behavior in thermo-mechanical contact.

REFERENCES

[1] D. Tabor, *The Hardness of metals*. Oxford University Press, 1951.

[2] K.L. Johnson, *Contact Mechanics*. Cambridge University Press, 1985.

[3] J.I. McCool, 'Comparison of models for the contact of rough surfaces', *Wear,* vol. 107, no. 1, pp. 37-60, 1986.

[4] M. Ciavarella, J.A. Greenwood and M. Paggi, 'Inclusion of "interaction" in the Greenwood and Williamson contact theory', *Wear*, vol. 265, no. 5-6, pp. 729-734, 2008.

[5] G.G. Adams and M. Nosonovsky, 'Contact modeling forces', *Tribology International*, vol. 33, no. 5-6, pp. 431-442, 2000.

[6] H. Zahouani and F. Sidoroff, 'Rough surfaces and elastoplastic contact', *Comptes Rendus de l'Académie des Sciences*, vol. 2, no. 5, pp. 709-715, 2001.

[7] J.A. Greenwoold and J.B.P. Williamson, 'Contact of normally flat surfaces', *Proceedings of the Royal Society of London. Series A*, vol. 295, pp. 300–318, 1966.

[8] H. Hertz, 'On the contact of elastic bodies', Journal of Reine Angew. Math. Vol. 92, pp. 156-171, 1881.

[9] J.A. Greenwood and J.H. Tripp, 'The Elastic Contact of Rough Spheres', *Journal of Applied Mechanics*, vol. 34, no. 1, p. 153, 1967.

[10] P.R. Nayak, 'Random process model of rough surfaces in plastic contact', *Wear*, vol. 26, no. 3, pp. 305-333, 1973.

[11] A.W. Bush, R.D. Gibson and T.R. Thomas, 'The elastic contact of a rough surface', *Wear,* vol. 35, no. 1, pp. 87-111, 1975.

[12] A.W. Bush, R.D. Gibson and G.P. Keogh, 'Strongly anisotropic rough surfaces', *Journal of Lubrication Technology*, vol. 101, no. 1, pp. 15-20, 1979.

[13] W.R. Chang, I. Etsion and D.B. Bogy, 'An elastic-plastic model for the contact of rough surfaces'. *Journal of Tribology*, vol. 109, no. 2, pp. 257-263, 1987.

[14] B. Bhushan, 'Contact mechanics of rough surfaces in tribology: Multiple asperity contact'. *Tribology Letters*, vol. 4, no. 1, pp. 1-35, 1998.

[15] B.N.J. Persson, O. Albohr, U. Tartaglino, A.I. Volokitin and E. Tosatti, 'On the nature of surface roughness with application to contact mechanics, sealing, rubber friction and adhesion', *Journal of Physics: Condensed Matter*, vol. 17, no. 1, pp. 1-62, 2005.

[16] F. Robbe-Valloire, B. Paffoni and R. Progri, 'Load transmission by elastic, elasto-plastic or fully plastic deformation of rough interface asperities', *Mechanics of Materials*, vol. 33, no. 11, pp. 617-633, 2001.

[17] F. Robbe-Valloire, R. Progri, B. Paffoni and R. Gras, 'Modelisation de la topographie microgeometrique et application à la prévision de l'écrasement', *12ème Colloque international: Méthodes d'investigations physicochimiques et mécanique des surfaces*, ERNS Mines ST ETIENNNE, 1999, p. 7.

[18] François Robbe-Valloire, 'Statistical analysis of asperties on a rough surface', *Wear*, vol. 249, no. 5-6, pp. 401-408, 2001.

[19] F. R-Valloire, B. Paffoni, R. Progri, 'Approche stochastique de l'analyse de contact statique entre surfaces rugueuses', *Tribologie et conception mécanique,* Saint-Quen*, France,* 2004, p. 155.

[20] S. Belghith, S. Meslini, H. BelhadjSalah and J.L. Ligier, 'Modeling of contact between rough surface using homogenization technique', *Comptes Rendus Mécanique*, vol. 338, no. 1, pp. 48-61, 2010.

[21] S. Hyun, L. Pei, J.F. Molinary and M.O. Robbins, 'Finite-element analysis of contact between elastic self-affine surfaces', *Physical Review E,* 70, 026117, 2004.

[22] L. Pei, S. Hyun, J.F. Molinari and M.O. Robbins, 'Finite element modeling of elasto-plastic contact between rough surfaces', *Journal of the Mechanics and Physics of Solids*, vol. 53, no. 11, pp. 2385-2409, 2005.

[23] P. Sahoo and N. Ghosh, 'Finite element contact analysis of fractal surfaces', *Journal of Physics D: Applied Physics*, vol. 40, no. 14, pp. 4245-4252, 2007.

[24] C. Mayeur, L. Flamand 'Modélisation du Contact Rugueux Elastoplastique'. *PhD thesis*, INSA Lyon, 1995.

[25] B. Buchner, M. Buchner and B. Buchmayr, 'Determination of the real contact area for numerical simulation', *Tribology International*, vol. 42, no. 6, pp. 897-901, 2009.

[26] E.J. Abbott and F.A. Firestone, 'Specifying surface quality: a method based on accurate measurement and comparison', *Mechanical Engineering*, vol. 2, no. 4, pp. 569-572, 1933.

[27] W. Peng and B. Bhushman, 'Three-dimensional contact analysis of layered elastic/plastic solids with rough surface', *Wear*, vol. 249, no. 9, pp. 741-760, 2001.

[28] M. Ciavarella, C. Murolo and G. Demelio, 'On the elastic contact of rough surfaces: Numerical

experiments and comparisons with recent theories', *Wear*, vol. 261, no. 10, pp. 1102-1113, 2006.

[29] A. Majumdar and B. Bhushan, 'Fractal model of elastic-plastic contact between rough surfaces', *Journal of Tribology*, vol. 113, no. 1, pp. 1-11, 1991.

[30] B.N.J. Persson, 'Theory of rubber friction and contact mechanics', *The Journal of Chemical Physics*, vol. 115, no. 8, pp. 3840-3861, 2001.

[31] B.N.J. Persson, 'Elastoplastic contact between randomly rough surfaces', *Physical Review Letters*, vol. 87, no. 11, pp. 1-4, 2001.

[32] A. Almqvist, C. Campana, N. Prodanov and B.N.J. Persson, 'Interfacial separation between elastic solids with randomly rough surfaces: Comparison between theory and numerical techniques', *Journal of the mechanics and physics solids*, vol. 59, no. 11, pp. 2355-2369, 2011.

[33] B.N.J. Persson, 'Contact mechanics for randomly rough surfaces', *Surface Science Reports*, vol. 61, no. 4, pp. 201-227, 2006.

[34] B.N.J. Persson, 'On the elastic energy and stress correlation in the contact between elastic solids with randomly rough surfaces', *Journal of Physics: Condensed Matter*, vol. 20, no. 3, pp. 1-3, 2010.

[35] D. Goerke and K. Willner, 'Normal contact of fractal surfaces-Experimental and numerical investigations', *Wear*, vol. 264, no. 7-8, pp. 589-598, 2008.

[36] M.B. Amor, S. Belghith and S. Mezlini, 'Finite Element Modeling of RMS Roughness Effect on the Contact Stiffness of Rough Surfaces', *tribology in industry*, vol. 38, no.3, pp. 392-401, 2016.

[37] W.W. Chen and Q.J. Wang, 'Thermomechanical analysis of elastoplastic bodies in a sliding spherical contact and the effects of sliding speed, heat partition and thermal softening', *Journal of Tribology*, vol. 130, no. 4, pp. 1-10, 2008.

[38] W.W. Chen, Q.J. Wang and W. Kim, 'Transient thermomechanical analysis of sliding electrical contacts of elastoplastic bodies, thermal softening, and melting inception', *Journal of Tribology*, vol. 131, no. 2, pp. 1-10, 2009.

[39] ISO 4287, Spécification Géométrique des Produits (GPS) Etat de surface: Terme et définition des paramètres d'état de surface, 1998.

[40] ISO 12085, Spécification Géométrique des Produits (GPS) Etat de surface: Méthode du Profil Paramètres liés aux motifs, 1998.

[41] H.C. Ward, 'Profile Characterization', *Rough Surfaces*, Edited by T. R. Thomas, Longman, London, pp. 72-88, 1982.

[42] American Petroleum Institue. *Specification for line pipe.* 2000.

[43] O. Chang-Kyun, 'A phenomenological model of ductile fracture for API X65 steel', *Internatinal Journal of Mechanical Science,* vol. 49, no. 12 pp. 1399-1412, 2007.

[44] C. Putignano, L. Afferrante, G. Carbone and G. Demelio, 'A new efficient numerical method for contact mechanics of rough surfaces', *International Journal of Solids and Structures,* vol. 49, no. 2, pp 338-343, 2012.

[45] S. Hyun, L. Pei, J.-F. Molinari and M.O. Robbins, 'Finite-element analysis of contact between elastic self-affine surfaces', *Physical Review E*, 70 026117, 2004.

[46] C. Mayeur, P. Sainsot and L. Flamand 'A numerical elastoplastic model for rough contact'. *Journal of Tribology,* vol. 117, no. 3, pp. 422–429, 1995.